

Thermodynamics of the 3D Hubbard model on approach to the Néel transition

Sebastian Fuchs,¹ Emanuel Gull,² Lode Pollet,^{3,4} Evgeny Burovski,⁵
 Evgeny Kozik,⁴ Thomas Pruschke,¹ and Matthias Troyer⁴

¹*Institut für theoretische Physik, Georg-August-Universität Göttingen, 37077 Göttingen, Germany*

²*Department of Physics, Columbia University, New York, NY 10027, USA*

³*Physics Department, Harvard University, Cambridge, Massachusetts 02138, USA*

⁴*Theoretische Physik, ETH Zurich, 8093 Zurich, Switzerland*

⁵*LPTMS, CNRS and Université Paris-Sud, UMR8626, Bâtiment 100, 91405 Orsay, France*

(Dated: October 22, 2018)

We study the thermodynamic properties of the 3D Hubbard model for temperatures down to the Néel temperature using cluster dynamical mean-field theory. In particular we calculate the energy, entropy, density, double occupancy and nearest-neighbor spin correlations as a function of chemical potential, temperature and repulsion strength. To make contact with cold-gas experiments, we also compute properties of the system subject to an external trap in the local density approximation. We find that an entropy per particle $S/N \approx 0.65(6)$ at $U/t = 8$ is sufficient to achieve a Néel state in the center of the trap, substantially higher than the entropy required in a homogeneous system. Precursors to antiferromagnetism can clearly be observed in nearest-neighbor spin correlators.

PACS numbers: 03.75.Ss, 05.30.Fk, 71.10.Fd

The Hubbard model [1] remains one of the cornerstone models in condensed matter physics, capturing the essence of strongly correlated electron physics relevant to high-temperature superconductors [2] and correlation driven insulators [3]. While qualitative features of the phase diagram are known from analytical approximations, controlled quantitative studies in the low-temperature regimes relevant for applications are not readily tractable with tools presently available. A recent program that aims to implement the Hubbard model in a cold gases experiment [4] has led to experimental signs of the Mott insulator [5, 6]. Modeling by dynamical mean field theory (DMFT) [6, 7] and high-temperature series expansions [8] resulted in temperature and entropy estimates and an error budget [9]. A major experimental achievement will be the detection of the antiferromagnetic phase, for which the slow and ill-understood equilibration rates, the limited number of detection methods, and inherent cooling problems will have to be overcome.

Experimental progress has also sparked interest in simulations of the 3D Hubbard model where new algorithms have been developed to treat the Hubbard model, such as the real-space DMFT [10, 11] or diagrammatic Monte Carlo [12] studies. Similar to the case of bosons, where synergy between experiment and simulation has led to quantitative understanding of experiments [13], accurate results for the thermodynamics of the 3D Hubbard model will also be crucial for validation, calibration and thermometry of fermionic experiments. A crucial role is played by the entropy, since these experiments form isolated systems where ideally the parameters are changed adiabatically (and not isothermally).

In this Letter we provide the full thermodynamical equation of state of the Hubbard model – in particular the entropy, energy, density, double occupancy and

spin correlations – for interactions U up to the bandwidth $12t$ on approach to the Néel temperature T_N by performing controlled large-scale cluster dynamical mean field calculations and extrapolations to the infinite system size limit, as well as determinantal diagrammatic Monte Carlo (DMC) simulations at half filling. We then use this information to calculate the entropy per particle required for experiments on ultracold atomic gases in optical lattices to reach a Néel state in the trap center. We finally show that the nearest-neighbor spin correlation function contains clear precursors for antiferromagnetism that may already be detectable in current generation experiments and that are useful for thermometry (more so than measurements of the double occupancy) close to T_N .

The Hubbard model is defined by its Hamiltonian

$$\hat{H} = -t \sum_{(i,j),\sigma} \hat{c}_{i\sigma}^\dagger \hat{c}_{j\sigma} + U \sum_i \hat{n}_{i\uparrow} \hat{n}_{i\downarrow} - \sum_{i,\sigma} \mu_i \hat{n}_{i\sigma}, \quad (1)$$

where $\hat{c}_{i\sigma}^\dagger$ creates a fermion with spin component $\sigma = \uparrow, \downarrow$ on site i , $\hat{n}_{i\sigma} = \hat{c}_{i\sigma}^\dagger \hat{c}_{i\sigma}$, $\langle \dots \rangle$ denotes summation over neighboring lattice sites, t is the hopping amplitude, U the on-site repulsion, and $\mu_i = \mu - V(\vec{r}_i)$ with μ the chemical potential and $V(\vec{r}_i)$ the confining potential at the location of the i -th lattice site. We will set $V(\vec{r}) = 0$ in all calculations and consider realistic traps later on.

Our numerical approach is a cluster generalization of dynamical mean field theory [14]. In cluster DMFT the self energy is approximated by N_c momentum-dependent basis functions $\phi_K(k)$: $\Sigma(k, \omega) \approx \sum_K^N \phi_K(k) \Sigma_K(\omega)$. The exact problem is recovered for $N_c \rightarrow \infty$. Within the dynamical cluster approximation (DCA)[15] used here, $\phi_K(k)$ are piecewise constant over momentum patches. The DMFT method [16] is the $N_c = 1$ cluster approximation where $\Sigma = \Sigma(\omega)$ and no momentum dependence is retained.

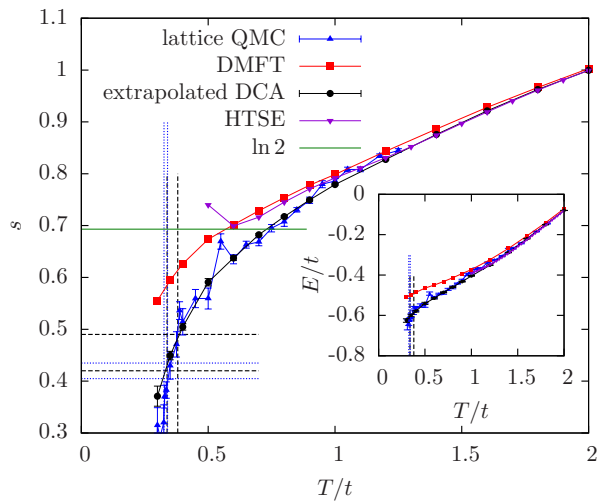


FIG. 1: (color online) Entropy per lattice site s of the Hubbard model as a function of temperature T/t , for $U/t = 8$, at half filling. Shown with dashed vertical lines is T_N from Ref. [21] (black) and with dotted lines according to DMC (blue). Shown with dashed horizontal lines is the entropy per lattice site s at T_N [21] (black), with dotted lines according to DMC (blue); also $\log(2)$ is shown as a full horizontal line (green). The inset shows the energy E per lattice site.

Solving the DMFT and DCA equations requires the solution of a quantum impurity model. Continuous-time quantum impurity solvers [17–19], in particular the continuous-time auxiliary field (CT-AUX) method used here [18], combined with advanced numerical techniques [20], have made it feasible to solve such models efficiently and numerically exactly on large clusters, thereby providing a good starting point for an extrapolation of finite size clusters to the infinite system [12, 21, 22]. We have performed extensive DCA calculations on bipartite clusters with $N_c = 18, 26, 36, 48, 56$, and 64. In order to achieve an optimal scaling behavior we exclusively use the clusters determined in Ref. [21] following the criteria proposed by [23]. As the DCA exhibits a $1/L^2$ finite-size scaling in the linear cluster size $L = N_c^{1/3}$ [24], we extrapolate our cluster results linearly in $N_c^{-2/3}$. Our error bars include extrapolation uncertainties. Despite a sign problem away from half-filling, temperatures $T/t \geq 0.4$, on the order of the Néel temperature, are reliably accessible for all but the largest interaction strength $U = 12t$ where we have been restricted to $T/t \geq 0.5$.

The potential energy, double-occupancy, and nearest-neighbor spin-spin correlation have been measured directly. The kinetic energy $E_{\text{kin}} = \sum_{n, \vec{k}} \epsilon(\vec{k}) G(\vec{k}, i\omega_n)$ has been calculated by summing $\epsilon(\vec{k})$, the bare-dispersion of the simple cubic lattice, and the single-particle Green function $G(\vec{k}, i\omega_n)$ over all momenta \vec{k} and Matsubara frequencies $i\omega_n$. The entropy S has subsequently been

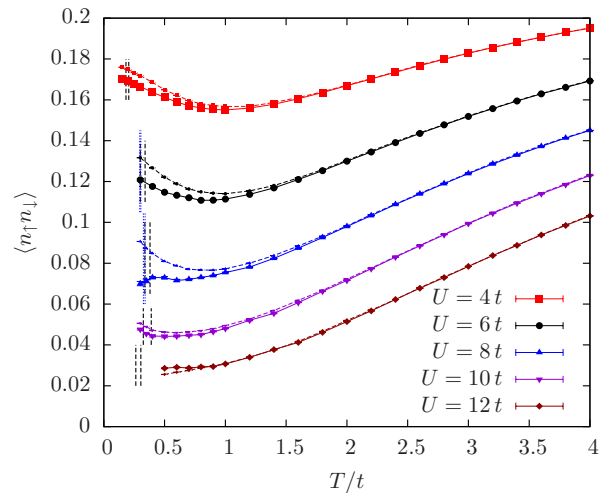


FIG. 2: (color online) Double occupancy of the Hubbard model as a function of temperature T , at half filling. Extrapolated DCA results are shown as solid lines and DMFT values as dashed lines. The vertical lines are the same as in Fig. 1.

calculated by numeric integration

$$S(T) = S(T_u) - \frac{E(T_u)}{T_u} + \frac{E(T)}{T} - \int_T^{T_u} dT' \frac{E(T')}{T'^2}, \quad (2)$$

up to a $T_u/t \approx 10$, where the entropy $S(T_u)$ is accurately given by a high-temperature series expansion. Tables of the complete results containing finite cluster and extrapolated values at and away from half filling for the entropy, energy, density, double occupancy, and spin correlations are given in the supplementary material [25].

Results at half filling – We start our analysis at half filling and focus on $U/t = 8$ where we can compare with results from DMC simulations [26] (and the more accurate [27]). We see in Fig. 1 that the entropy calculated using DCA and DMC coincides within error bars at all temperatures. Agreement with a 10th order high-temperature series expansion [8] is found down to $T/t \approx 1.6$. At that temperature also single site DMFT starts to deviate because that method misses short-range antiferromagnetic correlations. The Néel temperature was found to be $T_N/t \approx 0.36(2)$ in Ref. [21]. Our DMC calculations find it more accurately at $T_N/t = 0.333(7)$. Using DCA calculations, the critical entropy is $s \approx 0.46(2)$ for T_N according to Ref. [21], and $s := S/N_c \approx 0.41(3)$ with T_N according to the DMC. In the rest of the paper we will only use the T_N as determined by DMC but with entropies calculated by DCA (since away from half filling only entropies calculated by DCA are available).

The *double occupancy*, which has played a crucial role in optical lattice experiments [5, 6, 8, 29], is shown in Fig. 2 as a function of temperature at half filling for different values of U/t . While for small U/t a remarkable increase is seen on approach to T_N , only a plateau re-

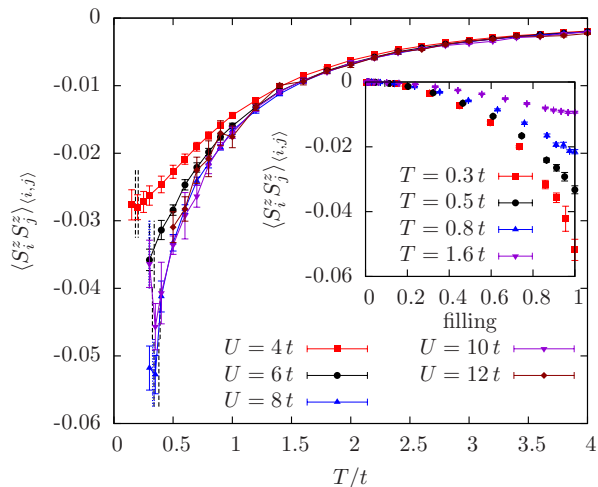


FIG. 3: (color online) Nearest-neighbor spin-spin correlation of the Hubbard model as a function of temperature T , at half filling. The inset shows the density dependency for $U/t = 8$ and selected temperatures. Vertical lines: compare to Fig. 1.

mains at moderate values of U/t . This is in contrast to the DMFT predictions, but similar to lattice QMC results in two dimensions [30]. For larger interactions ($U/t \gtrsim 12$), the double occupancy rises above that of a single site paramagnet, consistent with DMFT results for the anti-ferromagnetic phase below T_N [11]. The negative slope of $D(T)$, discussed in the context of single site DMFT [28], persists for a wide range of parameters. Sharp features just above T_N , as detected in single site (momentum independent) studies [11], are not observed for the interaction values and temperature ranges studied here. Hence the proposal that the double occupancy is a good candidate for thermometry is not substantiated by more accurate momentum-dependent calculations.

The *spin-spin correlation* function plotted in Fig. 3 as a function of temperature for various U and as a function of filling for $T/t = 0.3, 0.8$, and 1.6 at $U/t = 8$, is only accessible in methods that include non-local correlations, but may be accessible experimentally [31]. It has a steep slope on approach to the Néel temperature, which makes it an ideal quantity for thermometry. This corresponds to the intuitive picture that charge degrees of freedom are already essentially frozen out around T_N while the spin degrees of freedom start to order there.

Results away from half filling – Fig. 4 shows the entropy per lattice site for $U/t = 8$. The inset demonstrates that entropy per particle number N increases strongly at lower densities. While single site DMFT remains accurate for densities lower than $n \lesssim 0.6$ due to the weak momentum dependence of the self-energy in this regime [32], the DCA results are important for larger densities. Similarly, near half filling DMFT overestimates the double occupancy by 10%, while deviations are less pronounced at lower densities. This observation persists for all in-

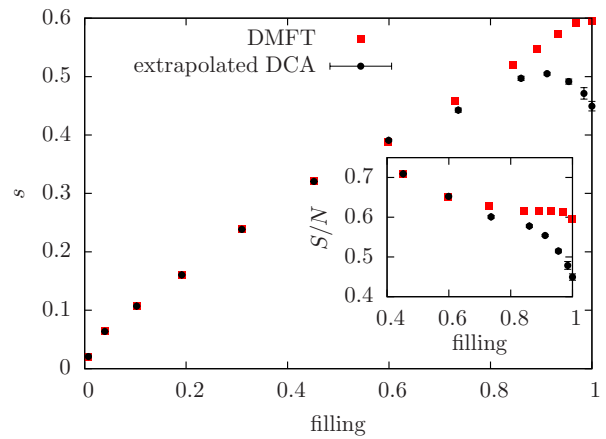


FIG. 4: (color online) Entropy per lattice site s and the entropy per particle S/N (inset) of the Hubbard model at the temperature $T = 0.35t \approx T_N$, as a function of density n , for $U/t = 8$. DMFT values and extrapolated DCA values are shown. The errors are dominated by extrapolation errors.

teractions and temperatures investigated. The flattening of the double occupancy for $8 \leq U/t \leq 12$ (cf. Fig. 2) is also seen away from half filling, and leads to virtually unchanged profiles over the trap in an optical lattice system. On the other hand, the spin-spin correlation function away from half filling (see the inset in Fig. 3) changes most rapidly near half filling when approaching the Néel temperature since it couples strongly to the developing (short-range) spin correlations.

Entropy in the optical lattice system – We now turn to the experimentally relevant case of an optical lattice in a harmonic trap, which is a closed system where entropy is conserved and temperature changes when adiabatically changing the parameters of the Hamiltonian. We choose parameters close to current experiments: $V(\vec{r}) = 0.004(|\vec{r}|/a)^2 t$ with lattice spacing a , and we consider the case of half filling in the trap center: $\mu = U/2$. We treat the harmonic confinement in a local density approximation(LDA): for every site we perform a DCA simulation for a homogeneous system and average the results over the trap. LDA was found to be a good approximation for the Bose-Hubbard model for wide traps, except in close proximity to the critical point [33–35] of the U(1) phase transition because of the diverging correlation length and in our setup errors due to the LDA can be neglected compared to our other systematic errors.

Due to the large volume fractions, the wings of the gas may capture more entropy than the center of the trap, even though the entropy per site is comparable to the one in the center (see Fig. 5). In fact, the entropy of the whole density range $0.1 < n < 0.9$ is large, and this opens the possibility to observe anti-ferromagnetic order in the trap center at an average entropy per particle over the trap which is about 50% larger than what could be expected from a homogeneous study. Optimal

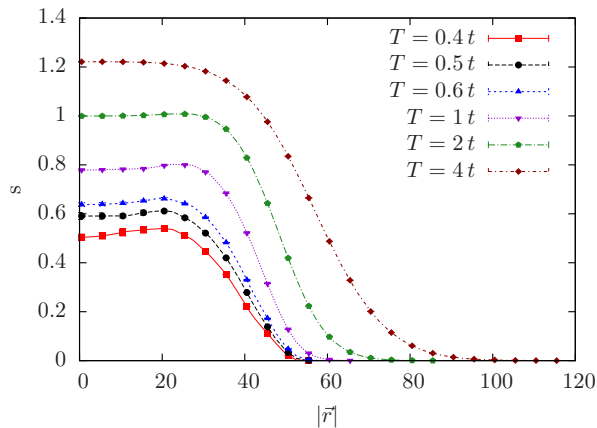


FIG. 5: (color online) Entropy profiles (entropy per lattice site) plotted over the trap in the LDA approximation for different temperatures with an interaction strength $U/t = 8$. Error bars are shown every 5 lattice spacings, but are generally smaller than the symbol size.

parameters are around $U/t = 8$ when $T_N/t = 0.333(7)$ according to DMC, corresponding to $S/N = 0.65(6)$ in the trap, while $S/N = 0.41(3)$ would be expected for a homogeneous system. As seen in Fig. 6, all U in the range $8 < U/t < 12$ lead to similar conclusions. We have verified that changing the trap by a factor of 4 does not alter these conclusions.

Conclusions – We have provided the full thermodynamics of the 3d Hubbard model using the DCA formalism for $U/t \leq 12$ and temperatures above the Néel temperature. Comparing to single site DMFT results we found that the latter already fail at remarkably high temperatures ($T/t \approx 1.5$ for $U/t = 8$ at the 1% level) near half filling. While the entropy per particle at the Néel temperature $T_N/t = 0.333(7)$ (determined with DMC) is $S/N = 0.41(3)$ for $U/t = 8$ in a homogeneously half filled system, we find that the Néel transition in a trap can already be reached at $S/N = 0.65(6)$ in a realistically sized harmonic trap (taking T_N according to Ref. [21] leads to $S/N = 0.69$).

We have also investigated the double occupancy and the nearest-neighbor spin-spin correlation function as quantities that are experimentally measurable and which were suggested to show precursors of antiferromagnetism. It turns out that the double occupancy is more or less flat as a function of temperature, while the spin correlations show a strong temperature dependence around the Néel temperature. This suggests that the spin correlations, not the double occupancy, are best suited to observe precursors of antiferromagnetism and measure the temperature. Our numerical data can be used to calibrate such a spin-correlation thermometer.

We acknowledge stimulating discussions with I. Bloch, T. Esslinger, A. Georges, D. Greif, O. Parcollet, V. Scarola, and L. Tarruell. This work was supported

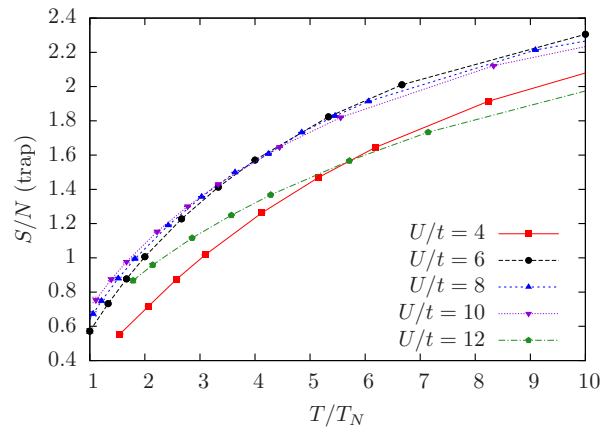


FIG. 6: (color online) Entropy per particle averaged over the trap as a function of temperature relative to the Néel temperature for different U . The Néel temperature is reached at $T/t = 0.333(7)$ for $U/t = 8$, when the average entropy is $S/N = 0.65(6)$. Errors (not shown) in $S(T_N)$ are estimated to be in the 10% range, with the largest contribution caused by the uncertainty in T_N .

by the Swiss National Science foundation, the National Science Foundation grants DMR-0705847 and PHY-0653183, grant no. ANR-BLAN-6238, the Aspen Center for Physics, a grant from the Army Research Office with funding from the DARPA OLE program, and by the Deutsche Forschungsgemeinschaft through the collaborative research center SFB 602. We used the Brutus cluster at ETH Zurich and computational resources provided by the Norddeutscher Verbund für Hoch- und Höchstleistungsrechnen (HLRN) and by the Gesellschaft für wissenschaftliche Datenverarbeitung Göttingen (GWDG). Simulation codes were based on the ALPS libraries [36].

-
- [1] J. Hubbard, Proc. Roy. Soc. (London), Ser. A **276**, 238 (1963).
 - [2] P. W. Anderson, Science **235**, 1196 (1987).
 - [3] M. Imada, A. Fujimori, and Y. Tokura, Rev. Mod. Phys. **70**, 1039 (1998).
 - [4] M. Köhl *et al.*, Phys. Rev. Lett. **94**, 080403 (2005).
 - [5] R. Jördens *et al.*, Nature (London) **455**, 204 (2008).
 - [6] U. Schneider *et al.*, Science **322**, 1520 (2008).
 - [7] L. De Leo *et al.*, Phys. Rev. Lett. **101**, 210403 (2008).
 - [8] V. W. Scarola *et al.*, Phys. Rev. Lett. **102**, 135302 (2009).
 - [9] R. Jördens *et al.*, Phys. Rev. Lett. **104**, 180401 (2010).
 - [10] M. Potthoff and W. Nolting, Phys. Rev. B **59**, 2549 (1999).
 - [11] E. V. Gorelik *et al.*, arXiv:1004.4857 (2010).
 - [12] E. Kozik *et al.*, Europhys. Lett. **90**, 10004 (2010).
 - [13] S. Trotzky *et al.*, arXiv:0905.4882v1, to appear in Nature Physics.
 - [14] T. Maier *et al.*, Rev. Mod. Phys. **77**, 1027 (2005).
 - [15] M. H. Hettler *et al.*, Phys. Rev. B **58**, R7475 (1998).

- [16] A. Georges *et al.*, Rev. Mod. Phys. **68**, 13 (1996).
- [17] A. N. Rubtsov, V. V. Savkin, and A. I. Lichtenstein, Phys. Rev. B **72**, 035122 (2005).
- [18] E. Gull *et al.*, EPL **82**, 57003 (2008).
- [19] P. Werner *et al.*, Phys. Rev. Lett. **97**, 076405 (2006); P. Werner and A. J. Millis, Phys. Rev. B **74**, 155107(2006).
- [20] E. Gull *et al.*, in preparation.
- [21] P. Kent *et al.*, Phys. Rev. B **72**, 060411(R) (2005).
- [22] T. Maier *et al.*, Phys. Rev. Lett. **95**, 237001 (2005);
- [23] D. D. Betts and G. E. Stewart, Can. J. Phys. **75**, 47 (1997).
- [24] T. Maier and M. Jarrell, Phys. Rev. B **65**, 041104 (2002).
- [25] see accompanying EPAPS document no. and the `aux` folder of the arXiv sources.
- [26] R. Staudt, M. Dzierzawa, and A. Muramatsu, Eur. Phys. J. B **17**, 411 (2000).
- [27] E. Burovski *et al.*, Phys. Rev. Lett. **101**, 090402 (2008).
- [28] F. Werner *et al.*, Phys. Rev. Lett. **95**, 056401 (2005).
- [29] N. Strohmaier *et al.*, Phys. Rev. Lett. **104**, 080401 (2010).
- [30] T. Pavia *et al.*, Phys. Rev. Lett **104**, 066406 (2010).
- [31] S. Trotzky *et al.*, arXiv:1009.2415 (2010).
- [32] E. Gull *et al.*, arXiv:1007.2592 (2010).
- [33] S. Wessel *et al.*, Phys. Rev. A **70**, 053615 (2004).
- [34] M. Campostrini and E. Vicari, Phys. Rev. Lett. **102**, 240601 (2009); Phys. Rev. A, **81**, 023606 (2010).
- [35] L. Pollet, N. V. Prokof'ev, and B. V. Svistunov, Phys. Rev. Lett. **104**, 245705 (2010).
- [36] A. F. Albuquerque, *et al.*, Journal of Magnetism and Magnetic Materials **310**, 1187 (2007).